Model for stathmin/OP18 binding to tubulin

Gerlind Wallon[1], Juri Rappsilber[2], Matthias Mann[2] and Luis Serrano

Structural Biology Program, EMBL, Meyerhofstrasse 1, 69117 Heidelberg, Germany and [2]Protein Interaction Laboratory, University of Southern Denmark, Campusvej 55, 5230 Odense, Denmark

[1]Corresponding author
e-mail: wallon@embl-heidelberg.de

Stathmin/OP18 is a regulatory phosphoprotein that controls microtubule (MT) dynamics. The protein does not have a defined three-dimensional structure, although it contains three distinct regions (an unstructured N-terminus, N: 1–44; a region with high helix propensity, H 1: 44–89; and a region with low helix propensity, H 2: 90–142). The full protein and a combination of H 1 and H 2 inhibits tubulin polymerization, while the combination of H 1 and the N-terminus is less efficient. None of the individual three regions alone are functional in this respect. However, all of them cross-link to α-tubulin, but only full-length stathmin produces high-molecular-weight products. Mass spectrometry analysis of α-tubulin–stathmin/OP18 and its truncation products shows that full-length stathmin/OP18 binds to the region around helix 10 of α-tubulin, a region that is involved in longitudinal interactions in the MT, sequestering the dimer and possibly linking two tubulin heterodimers. In the absence of the N-terminus, stathmin/OP18 binds to only one molecule of α-tubulin, at the top of the free tubulin heterodimer, preventing polymerization.
Keywords: cross-linking/mass spectrometry/OP18/stathmin/tubulin

Introduction

The microtubule (MT) cytoskeleton plays a wide variety of structural and functional roles in cells, including maintenance of cell shape, intracellular transport, organization of the spatial distribution of organelles in the cytoplasm, cell polarity and chromosome segregation during mitosis (for a review, see Cole and Lippincott-Schwartz, 1995). The characteristic property of MTs, known as dynamic instability, involves rapid transitions between polymerization and depolymerization of α- and β-tubulin heterodimers from the ends of MTs. The MT dynamics are regulated by microtubule-associated proteins (MAPs), which favour MT polymerization, thereby stabilizing the MTs. MAP phosphorylation weakens the stabilizing effect, presumably by decreasing their affinity toward MTs (for a review, see Hirokawa, 1994). However, MAPs alone do not account for the regulation of MT dynamics during the cell cycle. An analysis of MT dynamics in intact cells suggests the presence of MT regulatory factors that oppose the action of MAPs by inducing depolymerization, also termed catastrophe (Drechsel *et al.*, 1992). More recently another type of cellular factor has been identified that destabilizes MTs *in vitro* and in intact cells (Belmont and Mitchison, 1996). These proteins are encoded by the stathmin gene family (Maucuer *et al.*, 1993). Stathmin/OP18 [also termed oncoprotein 18 (OP18), p19, metablastin and prosolin] is a ubiquitous, well-conserved, cytosolic phosphoprotein. Stathmin/OP18 has been detected in all tissues, the highest levels being found in brain, neurons, testis and leukemic lymphocytes. Expression and phosphorylation are modulated by a diverse number of extracellular signals. The phosphorylation state varies during the cell cycle and peaks during mitosis (Marklund *et al.*, 1993). Stathmin/OP18 is phosphorylated on up to four serine residues by different kinases. The known phosphorylation sites are Ser16, Ser25, Ser38 and Ser63.

Stathmin/OP18 has been shown to interact directly with MTs (Belmont and Mitchison, 1996). A complex of one stathmin/OP18 molecule binding two tubulin heterodimers (T_2S complex) was detected using analytical ultracentrifugation (Jourdain *et al.*, 1997) and by gel filtration chromatography (Curmi *et al.*, 1994). This interaction is directly dependent on the degree of phosphorylation of stathmin/OP18, where increasing phosphorylation inhibits binding to tubulin (Horwitz *et al.*, 1997; Larsson *et al.*, 1997). Cross-linking of tubulin with stathmin/OP18 phosphorylated in varying combinations at the four phosphorylation sites shows that phosphorylation on Ser16 and Ser63 has the strongest effect on tubulin binding. In conjunction with results from biochemical and genetic experiments, those authors propose a model stating that dual phosphorylation on the cyclin-dependent kinase (CDK) sites Ser25 and Ser38 is required for phosphorylation of Ser16 and/or Ser63, but phosphorylation on the CDK sites alone is not sufficient to downregulate stathmin/OP18 activity.

The binding constant of stathmin/OP18 to tubulin is only micromolar (Curmi *et al.*, 1997), which is in agreement with the intracellular concentration of tubulin, which is also in the micromolar range.

Two possible mechanisms have been proposed to explain the destabilization of MTs by stathmin/OP18: (i) sequestration of the tubulin heterodimers, and thus depletion of the pool of tubulin available for polymerization (for a recent review, see Andersen, 1999); and (ii) catastrophe stimulation as proposed originally by Belmont and Mitchison (1996). Recently Howell *et al.* (1999) have tried to distinguish between these mechanisms, and found that stathmin/OP18 has a dual functional activity supporting both mechanisms, which are dependent on the pH. They found tubulin-sequestering and catastrophe-enhancing activity at pH 6.8, and a catastrophe-enhancing but no sequestering activity at pH 7.5.

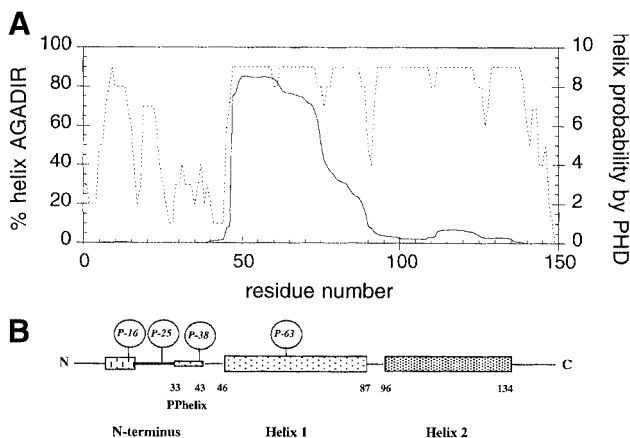We investigated how stathmin/OP18 and the tubulin

A

B

Fig. 1. Secondary structure prediction of stathmin/OP18. Stathmin/OP18 is a 149-amino-acid protein with four consensus serine phosphorylation sites. (**A**) The secondary structure prediction by PHD predicts a mainly helical protein (dotted line). The N-terminus is relatively unstructured, followed by a long helical stretch interrupted at residues 87–94. Helix calculation by AGADIR predicts a strong helix between residues 46 and 78 only. We have identified a possible PPII helix between the N-terminus and the first helix. The helical region has coiled-coil-forming potential. (**B**) Model of the secondary structure elements and phosphorylation sites of stathmin/OP18. The protein is divided into three parts: N-terminus, helix 1 and helix 2.

Fig. 2. Far-UV CD spectrum of a peptide with the sequence of the proposed PPII helical segment of stathmin/OP18 (continuous line) and a control peptide with the signature sequence destroyed (dotted line). The peptide sequences are YG**P**EF**P**LS**PP** as the original stathmin/OP18 sequence and YG**P**EFGLS**PP** as the control. The N-terminal tyrosine was added in order to be able to determine peptide concentration. The PPII-typical signature of the original stathmin/OP18 peptide is much stronger than that of the control, which indicates PPII-like conformation.

heterodimer bind to each other. Stathmin/OP18 is composed of three secondary structure elements, which were expressed separately and assayed for their effect on tubulin polymerization. All three secondary structure elements (truncations) were tested for their capability to cross-link with the tubulin heterodimer in the presence of a chemical cross-linker. In order to determine the site of interaction between the proteins, we analysed the cross-linked and completely proteolysed complex of stathmin/OP18 or its truncations with tubulin by mass spectrometry. We found that the two predicted helices of stathmin/OP18 bind to the region around helix 10 of α-tubulin. In the truncated versions of stathmin/OP18, helix 1 binds to a region between helix 4 and strand 5 of α-tubulin. A structural and functional model is suggested for this interaction.

Results

Structure prediction

The secondary structure prediction method PHD has a success score >70% on average when several related sequences are available (Rost *et al.*, 1994). Prediction for the stathmin/OP18 family indicates that there are three regions in terms of secondary structure: a relatively unstructured N-terminus with a potential polyproline II (PPII) helix at its end, followed by two highly charged helices (helices 1 and 2; Figure 1B). These two α-helices, termed H 1 and H 2, additionally have a coiled-coil-forming potential (COILS; Lupas *et al.*, 1991; Maucuer *et al.*, 1995). The helical content in aqueous solution of monomeric peptides in the absence of tertiary interactions can be estimated by the algorithm AGADIR (Muñoz and Serrano, 1994; Lacroix *et al.*, 1998). AGADIR predicts a strong helical propensity for H 1 (47% helical), while H 2 is predicted to have low helical propensity (17% helical) and the N-terminus is essentially unstructured from the helical point of view (3% helical) (Figure 1A). This
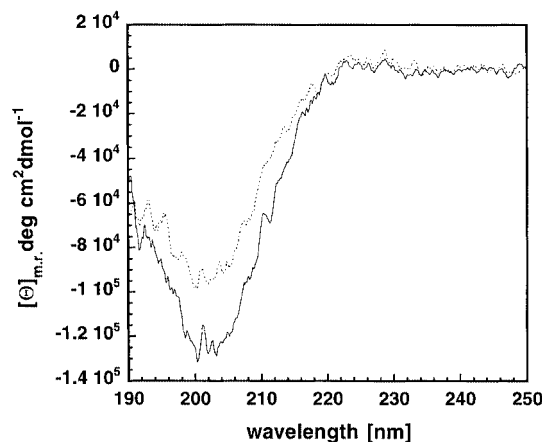
indicates that the region corresponding to H 1 will, to a large extent, be populating the α-helical conformation in aqueous solution in the absence of contacts with the rest of the protein, while H 2 will be largely unstructured. Sequence analysis also reveals a possible PPII segment close to the N-terminus of α-helix 1 (Figure 1B). The PPII helix structure is characterized by a repetition every three elements and is induced by the presence of several proline residues in a sequence segment. More importantly, when several proline residues are present the PPII conformation is produced in the absence of tertiary contacts (Williamson, 1994).

Analysis of the proposed polyproline II segment

We have investigated the presence of the PPII conformation by comparing a far-UV spectrum of a peptide with the stathmin/OP18 PPII sequence with that of a peptide of the same sequence but with one of the prolines substituted by a glycine, which would disrupt the PPII-typical sequence and conformation. The spectra were recorded under identical conditions at 4°C and corrected for concentration (Figure 2). The spectrum has the typical signature of a PPII conformation, with a maximum around 228 nm and a minimum around 201 nm (Viguera *et al.*, 1994; Pisabarro and Serrano, 1996). The higher intensity signal of the proposed polyproline-containing peptide as compared with the control indicates that this part of stathmin/OP18 can indeed take up a PPII helical conformation.

Cloning, expression and purification

Following the secondary structure analysis, we defined three regions in the stathmin/OP18 molecule: the N-terminus (1–43), helix 1 (44–89) and helix 2 (90–142). We cloned each secondary structure element separately as well as the consecutive combinations of N-terminus and helix 1 (N+H 1) and helices 1 and 2 (H 1+H 2). In all cases we were able to express and purify the constructions, except in the case of the N-terminal region alone.
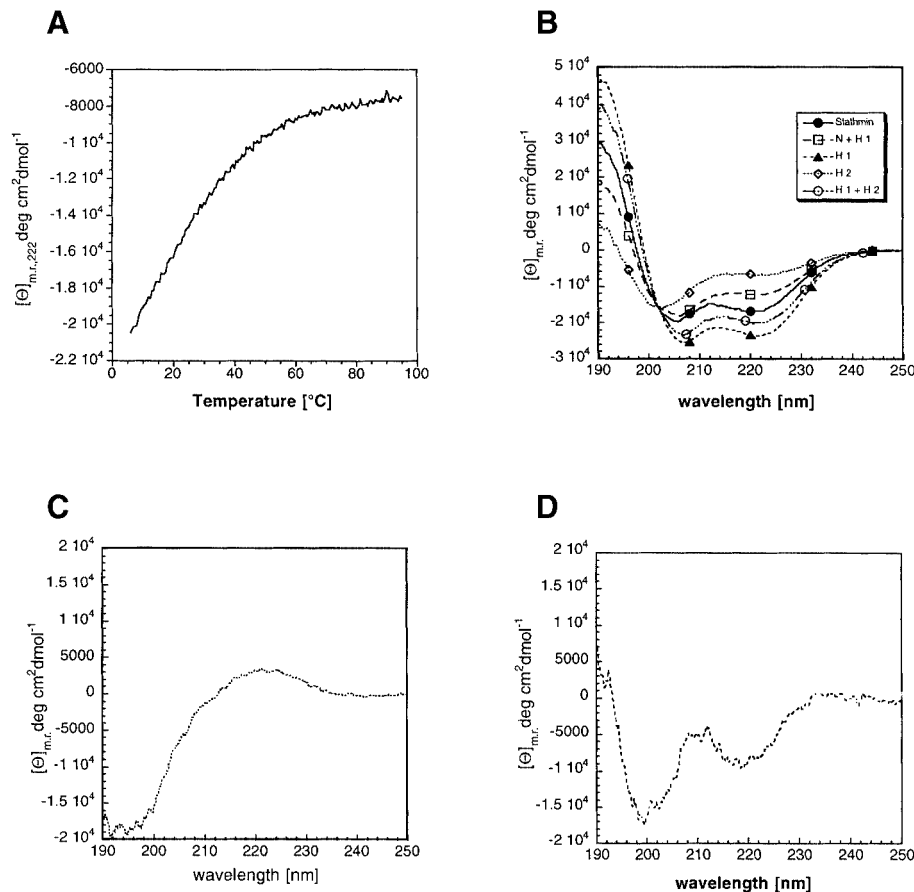
Fig. 3. Far-UV CD spectra of recombinant human stathmin/OP18 and its truncation products. (**A**) Thermal melting curve recorded at 222 nm. Stathmin/OP18 (0.1 mg/ml) is in 50 mM sodium phosphate pH 7.0. (**B**) Mean residue ellipticity of holo-stathmin/OP18 and its truncation products. (**C**) Theoretical spectrum of the N-terminus calculated by subtracting the spectrum of helix 1 from that of (N+H 1). The resulting spectrum represents a random coil. (**D**) Theoretical spectrum of the N-terminus calculated by subtracting the spectrum of truncation (H 1+H 2) from that of stathmin/OP18. The resulting spectrum has some helical signal.

CD analysis

We compared the CD spectra of stathmin/OP18 and its truncation products (Figure 3B). The whole protein presents a typical α-helical spectrum with a helix content of ~43% [calculated according to the method of Chen *et al.* (1974)]. More interestingly, the α-helix content of H 1 (62%) is higher than that of the full protein, while H 2 shows a low helix content (17%). These data agree with the helical tendency predicted by AGADIR. Comparison of the CD spectra of H 1 and H 2 separately with truncation (H 1+H 2) indicates that the combined truncation products have a larger helical content than the simple addition of the individual CD spectra, or AGADIR, would predict (52% helix versus a calculated helicity value assuming additivity of 38%). This could be due to mutual stabilization of the helical content of the two truncation products.

Since we could not express the N-terminus alone, we calculated its spectrum by subtracting the spectrum of H 1 from that of N+H 1 (Figure 3C). Alternatively, the spectrum of the N-terminus can also be calculated by subtracting the spectra of truncation (H 1+H 2) from that of full-length stathmin/OP18 (Figure 3D). In principle, if the resulting spectra are different this will indicate that the presence of H 2 affects the conformation of H 1. We found that in the first case the result is a random coil spectrum (Figure 3C). This agrees with the 3% helix

content predicted by AGADIR for the N-terminus alone, although there is always the question to what extent we can consider that the spectra of the two truncations will be strictly additive. However, this objection does not preclude the comparison with the other subtraction spectrum, since in both cases we always miss the N-terminus. In the case of the comparison between (H 1+H 2) and full-length stathmin/OP18, the resulting spectrum shows some residual helix content (Figure 3D). Therefore, it seems that the presence of H 2 results in a conformational change in the N-terminal region, suggesting the presence of some long-range interactions.

Thermal denaturation

We measured the thermal denaturation of stathmin/OP18 from 4 to 95°C (Figure 3A). Stathmin/OP18 does not behave as expected for a globular protein. For a folded protein with a distinct tertiary structure, a curve of sigmoidal shape is expected, due to the cooperative nature of protein denaturation. Here, stathmin/OP18 behaves like a peptide, i.e. there is not a single well-defined three-dimensional structure but rather an ensemble of conformations in equilibrium. The lack of cooperative behaviour in stathmin/OP18 is not due to protein aggregation, since the CD spectrum after heating and subsequent cooling is identical to that before heat treatment (data not shown).
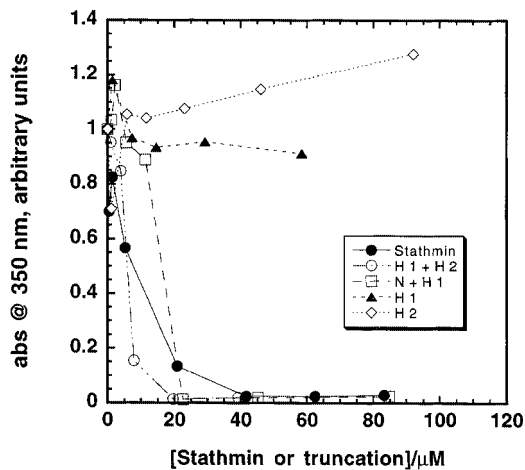
Fig. 4. Inhibition of tubulin polymerization by stathmin/OP18 and its truncation products. Bovine brain tubulin in BRB80 (5.8 mg/ml) and 33% glycerol were polymerized in the presence of different concentrations of stathmin/OP18 or its truncation products at 37°C. The end point of polymerization was recorded at 350 nm.

We know from the literature (Belmont and Mitchison, 1996) and our own assays (data not shown) that the activity of stathmin/OP18 is heat resistant. The poor dispersion of the lines in a one-dimensional NMR spectrum also suggests that the protein is not folded (data not shown). Together these data lead to the conclusion that stathmin/OP18 is not folded in isolation but could take up a defined tertiary structure upon binding to tubulin or other proteins.

Effect of stathmin/OP18 and its truncation products on microtubule assembly

Spontaneous polymerization of tubulin into MTs was inhibited efficiently by stathmin/OP18 and some of its truncation products. Figure 4 shows that full-length stathmin/OP18 and the truncation comprising helices 1 and 2 (H 1+H 2) were equally efficient in inhibiting tubulin polymerization, followed by the truncation comprising the N-terminus and helix 1 (N+H 1). The helices by themselves had only a very small effect on polymerization in the concentration range studied. The fact that truncation (H 1+H 2) and truncation (N+H 1) are sufficient for inhibiting tubulin polymerization indicates that each subdomain of stathmin/OP18 can interact independently with the tubulin molecule.

Cross-linking of the tubulin heterodimer and stathmin/OP18 and its truncation products

Previous studies have shown that stathmin/OP18 forms mainly a complex with α-tubulin upon chemical cross-linking with the zero-length cross-linker 1-ethyl-3-3-(dimethylamino)propylcarbodiimide (EDC) (Larsson *et al.*, 1997; Moreno *et al.*, 1999). N-terminal sequencing of the cross-linked complex indicated that 80–90% of the tubulin cross-linked to stathmin/OP18 is α-tubulin and 10–20% is β-tubulin (Larsson *et al.*, 1997). We studied the binding of the stathmin/OP18 truncation products to the tubulin heterodimer using the same chemical cross-linker. The truncation products were added at the same molar concentration as the full-length stathmin/OP18. As a control, to exclude non-specific cross-linking effects, two proteins
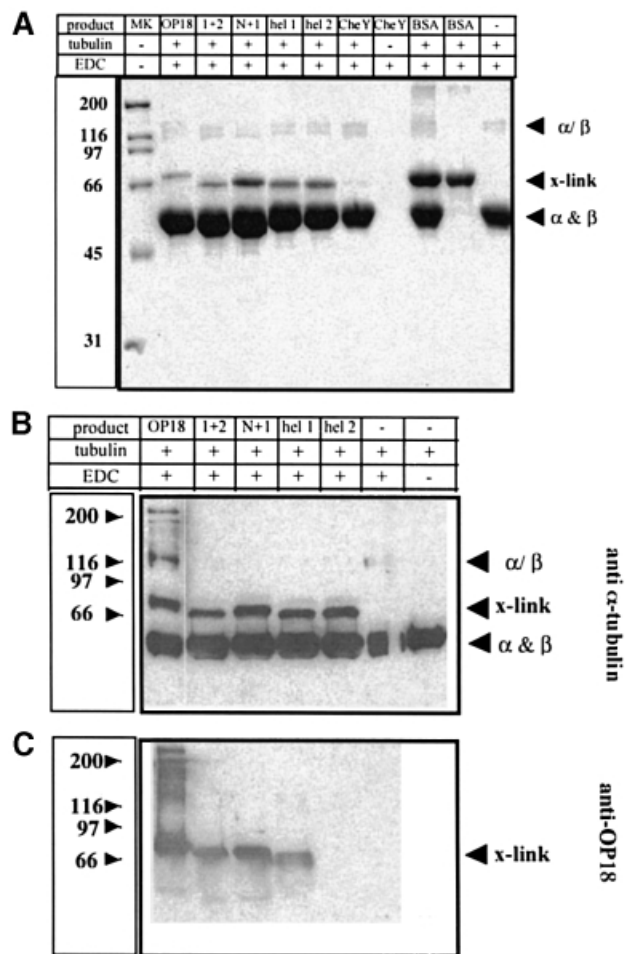

Fig. 5. Cross-linking of stathmin/OP18 or its truncation products with tubulin revealed by a zero-length cross-linker. Bovine brain tubulin (11.6 μM) and stathmin/OP18 (or its truncations, 6 μM) were incubated at 4°C for 1 h. The complex was cross-linked with EDC for 30 min at room temperature. The complexes were analysed by Coomassie-stained SDS–PAGE gels or by Western blotting. The positions of α- and β-tubulin and the specific complexes formed are indicated. Positions of the molecular weight standards are given on the left. (**A**) Coomassie-stained 12% SDS–PAGE gel. (**B**) Western blot of a 10% SDS–PAGE gel stained with an anti-α-tubulin antibody. (**C**) Western blot of a 10% SDS–PAGE gel stained with an anti-stathmin/OP18 antibody.

that should not interact with tubulin were cross-linked under the same conditions [bovine serum albumin (BSA) and a chemotactic protein from *Escherichia coli* CheY].

We found that all the stathmin/OP18 fragments tested cross-link to tubulin (Figure 5). Under the same conditions BSA did not cross-link to tubulin, while there was some minor cross-linking to CheY (Figure 5A). In all the cases a band corresponding to the molecular weight of the tubulin dimer was found. A Western blot was probed with an anti-α-tubulin antibody, an anti-β-tubulin antibody and an anti-stathmin/OP18 antibody. All antibodies recognized the cross-linked products (Figure 5B and C, with the exception of H 2, which does not contain the epitope against which the anti-stathmin/OP18 antibody was raised). The fact that the anti-β-tubulin antibody also recognizes the cross-linked products is expected (data not shown) since as was mentioned above 10–20% of the cross-linking of stathmin/OP18 is to β-tubulin.

Interestingly, additional higher molecular weight products involving stathmin/OP18 and tubulin were only detected in the cross-link of the full-length protein with tubulin. These products may represent the $T\alpha_2S$ complex postulated by Curmi *et al.* (1997) and Jourdain *et al.* (1997), and higher order complexes such as $T(\alpha\beta)_2S$ or T_3S (Larsson *et al.*, 1999). The fact that it only occurs with the full-length protein and not with any of the truncations indicates that all elements of stathmin/OP18 are necessary for T_2S and higher order complex formation.

Determination of stathmin/OP18–α-tubulin binding sites

Moreno *et al.* (1999) have narrowed down the site of interaction between stathmin/OP18 and α-tubulin to the C-terminal residues 307–417. This area comprises residues far away in the three-dimensional structure of tubulin (Nogales *et al.*, 1998) and therefore does not allow the postulation of a model for the inhibition of tubulin polymerization by stathmin/OP18. To define the site of interaction between the two proteins more closely we used an approach involving a combination of mass spectrometry and chemical cross-linking. In short, the previously described EDC-cross-linked tubulin–stathmin/OP18 complex, as well as those complexes between tubulin and stathmin/OP18 truncations, were separated from their constituents and high-molecular-weight by-products by SDS–PAGE and subsequently electroeluted from unstained gel slices. The samples were completely proteolysed by either trypsin (cleaves C-terminal of arginine and lysine) or Endo-LysC (cleaves C-terminal of lysine only). The chemical cross-linker EDC specifically links lysine with either aspartate or glutamate. Stathmin/OP18, its truncation products and tubulin were independently subjected to the same chemical reaction, or left uncross-linked, and digested as controls. The masses of the fragments were determined using MALDI-TOF MS. The controls were used to separate the fragments corresponding to uncross-linked stathmin/OP18/truncations and tubulin, as well as any internal cross-links within these two proteins, from those corresponding to stathmin/OP18/truncations-tubulin cross-linked fragments (Figure 6). The intensity of corresponding peaks in different MALDI mass spectra can vary to a considerable extent owing to the choice of matrix (Cohen and Chait, 1996) and suppression effects. For this reason samples have been analysed from both α-cyano-4-hydroxy-*trans*-cinnamic acid and 2,5-hydroxybenzoic acid. Only those peaks found in spectra recorded for the cross-linked dimer but not found in any of the spectra recorded for the unmodified or modified monomers were considered as candidates for cross-linked peptides and used for the comparison with the model. Because of the uncertainties associated with interpreting peak heights between different spectra it is essential that cross-link information be deduced only in a statistical manner from a set of candidates obtained from many different measurements. Peaks coinciding with known keratin contaminations have been excluded from the list of candidates.

To identify the cross-linked sequences a program developed by one of the authors (MASA; L.Serrano) was employed. This program determines the masses of all the fragments produced by a protease in the presence of a specific cross-linking agent, taking into account partial
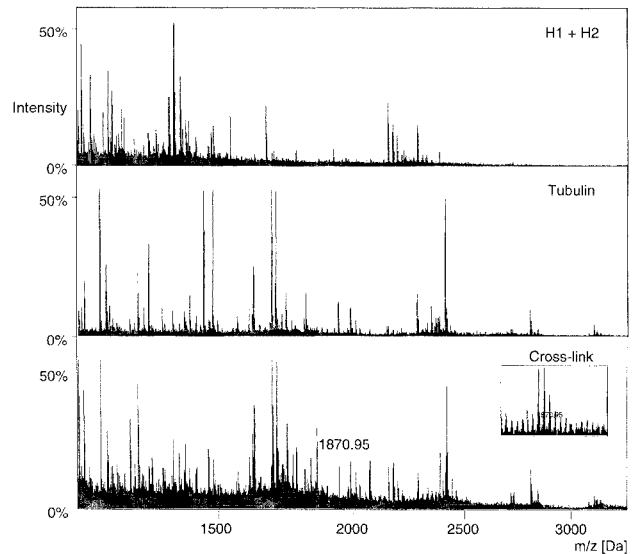

Fig. 6. MALDI mass spectra of truncation H 1+H 2, a mixture of α/β-tubulin, and the cross-linked product. Spectra were recorded using α-cyano-4-hydroxy-*trans*-cinnamic acid as the matrix. The labelled peak corresponds to candidates for cross-linked peptides.

digestion products. It searches for non-cross-linked and all possible inter- and intra-molecule cross-links that will render the experimentally determined mass within a given margin of error.

Tubulin purified from mouse brain was used for this study since the sequences of all isomers of α-tubulin from this organism are available from the database, whereas no sequence information is available for the most commonly used bovine brain tubulin. Tubulin isomers are more or less tissue specific, e.g. mouse tubulin α3/7 is specific for testis, whereas all other isomers can be found in different proportions or as trace amounts in different kinds of tissues (Villasante *et al.*, 1986). The major isomers in brain are α1 and α2. The small differences in amino acid sequence (e.g. α1 and α2 differ only at position 232) are detectable with mass spectrometry and it is therefore necessary to take all possible isomers into account in the analysis. The differences between the four known α-isomers encompass only very few amino acids and reside mainly in the 10 C-terminal residues, which are highly postranslationally modified in the cell (Redeker *et al.*, 1994, 1998; Vinh *et al.*, 1999). Apart from the known addition and elimination of a tyrosine at the C-terminus of α-tubulin, the rest of the chemical modifications occurring at the C-terminal regions are quite heterogeneous. Therefore, except for the extra tyrosine residue, we cannot take into consideration these modifications and will miss any cross-linking of stathmin/OP18 to the C-terminus of tubulin.

The results from the MALDI-TOF-MS analysis of the digested fragments are shown in Table I. The full-length stathmin/OP18–tubulin cross-links only were additionally digested with Endo-LysC.

In the analysis of the full-length stathmin/OP18–tubulin complex nine peaks were identified in the Endo-LysC digest, of which five were matched with possible stathmin/OP18–tubulin cross-links by the program. In the trypsin digest of the full-length stathmin/OP18–tubulin complex 12 peaks were identified, three of which correspond to

Table I. Masses from mass spectroscopy and possible cross-linked fragments calculated by MASA between stathmin/OP18 or its truncations and tubulin

Mass from measurement	Digestion enzyme	Δ to calc. mass	Mouse tubulin	Stathmin/OP18
1638.85	**T**	0.08	162–165	84–92 (H1 + H2)[h1]
		0.0	155–163	121–127 (H1 + H2)
1674.77	**T**	**0.11**	**155–162**	**69–77 (H1)**[h1]
1870.95	**T**	0.12	(α4) 325–338	133–136 (**H1** + H2)[H2]
		0.1		61–69, 131–136
2765.24	**T**	0.19	155–165	102–116
		0.13	307–319	36–48
		0.16	337–351	102–111[H2]
4368.60	**T**	0.19	214–242	59–69
		0.23	325–335	59–87[H1]
2196.25	**L**	**0.05**	**(α4) 325–335**	**59–69**[H1]
3540.99	**L**	0.06	325–337	116–135[H2]
		0.03		69–82, 126–142
3591.64	**L**	**0.11**	**303–325**	**102–111**[H2]
3606.58	**L**	**0.21**	**303–325**	**60–69**[H1]
3623.69	**L**	0.11	303–310	87–111[H2]
		0.11		50–60, 135–156

T, trypsin digest; L, Endo-LysC digest. The tubulin isomers in the cross-linked fragments are α1 and α2 unless noted otherwise. The numbering of Stathmin/OP18 includes the residues added by the His-tag. Unique fragments are in bold. Fragments used for the model are denoted according to their location on tubulin: [H2]H2 on the MT outside; [H1]H1 on MT inside; [h1]H1 at the 155–165 loop.

masses that match common keratin contaminants and two could be matched to possible cross-linked fragments. In total, seven peaks were found that correspond to possible cross-linked fragments of the full-length α-tubulin–stathmin/OP18 complex within the margin of error of the measurement (~0.01% of the molecular weight measured, 100 p.p.m.). Of these seven fragments, three are unique, corresponding to a single combination of stathmin/OP18 and α-tubulin: α-tubulin 325–335 with 59–69 (H 1) of stathmin/OP18, α-tubulin 303–325 with 60–69 (H 1) of stathmin/OP18 and the same tubulin fragment with region 102–111 (H 2) of stathmin/OP18. In the five remaining cases there is more than one fragment combination fitting the experimental mass. In two of them, one combination explaining the experimental mass involves homo-cross-linking of tubulin, or stathmin/OP18. However, the homo-cross-links of tubulin could be eliminated due to their physical impossibility (data not shown).

The analysis of the truncation products cross-linked to tubulin yielded eight possible masses, of which one mass matches a possible keratin contaminant and four masses correspond to possible cross-linked fragments, one of which is unique. This unique fragment identifies H 1 of stathmin/OP18 cross-linked to α1/2-tubulin 155–165. The masses derived from H 2 and N+H 1 yielded no possible cross-links. See Table I and Figures 7 and 8, residue numbers in stathmin/OP18 include the nine residues added by the His-tag.

Discussion

Stathmin/OP18 does not have an ordered tertiary structure

The data obtained by CD agree with the secondary structure prediction by PHD (Rost *et al.*, 1994) in that the structure of stathmin/OP18 is mainly helical even though there are large differences in the helicity of the two main helices. The spectra obtained from the single components
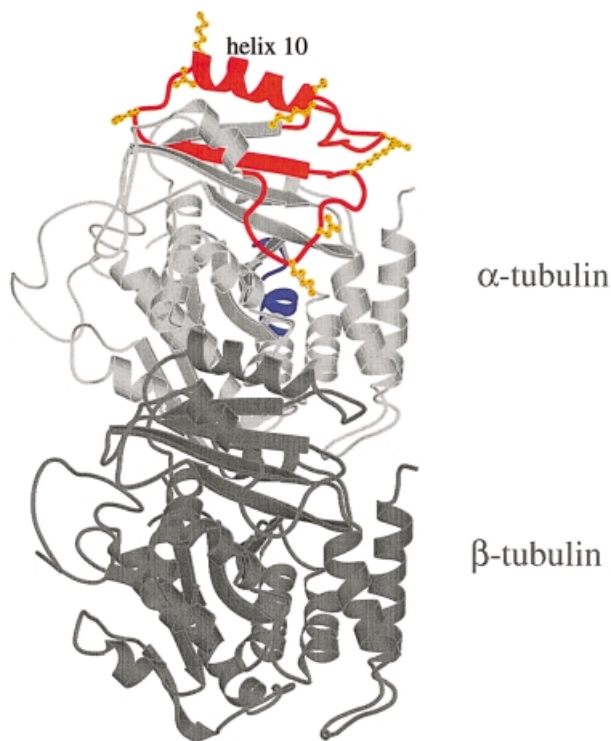

Fig. 7. The αβ-tubulin heterodimer (PDB accession code 1TUB). The fragments of α-tubulin that have been found to cross-link to stathmin/OP18 are marked in red. The lysines, aspartates and glutamates within these fragments that could furbish the actual cross-links to stathmin/OP18 are in orange. The fragment 155–165 from α-tubulin is marked in blue [the figure has been generated with MOLSCRIPT (Kraulis, 1991)].

are in reasonable accordance with the prediction of the helical propensities by AGADIR (Figures 1 and 3). In combination with the holo-protein, or H 1, the helical tendency of H 2 does seem to be higher than in isolation. In fact, it has been shown that segments of proteins
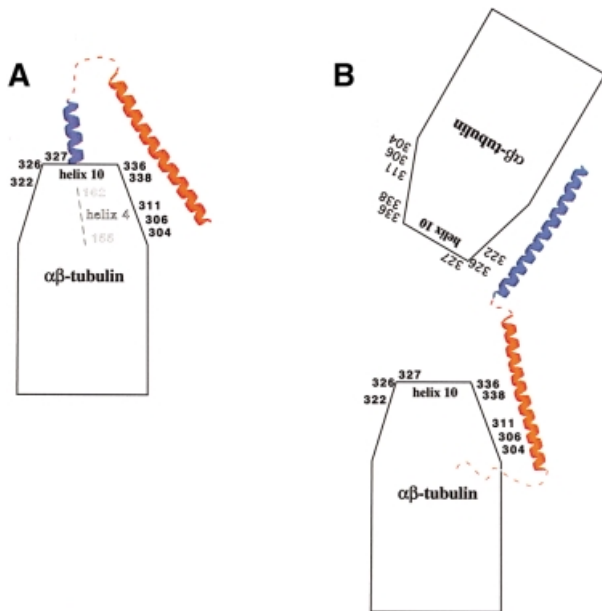
Fig. 8. Model for the interaction of stathmin/OP18 with α-tubulin. (**A**) The truncated forms of stathmin/OP18 bind only to one α-tubulin of the heterodimer. H 1 binds to H4–B5 (155–162) of α-tubulin, a region involved in lateral contacts between filaments. H 2 of stathmin/OP18 binds around helix 10 of α-tubulin. (**B**) For the complete molecule of stathmin/OP18 binding of H 1 to α-tubulin changes. H 1 binds close to the opposite side of helix 10 of α-tubulin, in such a manner that two heterodimers are connected by one molecule of stathmin/OP18.

predicted to be >10% helical in isolation by AGADIR are helical in a protein context (L.Serrano, unpublished data), as seems to be the case here. In the thermal melting there is no cooperativity in the unfolding of the protein, showing that there are only weak or no tertiary interactions, i.e. no distinct tertiary fold. However, there must be some long-range interactions, as shown by the finding that the CD spectra of the single and combined components of stathmin/OP18 are not the same when different combinations are used, which indicates that they do influence one another structurally. This is particularly obvious when comparing the two difference CD spectra that were calculated for the N-terminus (Figure 3C and D). When all three regions of stathmin/OP18 are present in the protein we obtain a partly helical spectrum for the N-terminus. In the absence of H 2 the difference spectrum appears like a random coil spectrum. This leads to the conclusion that there is some degree of long-range cross-talking between H 2 and the N-terminal domain. However, stathmin/OP18 is relatively unstructured in solution and it could acquire its active conformation upon binding to the tubulin heterodimer. In fact there are examples in the literature for this kind of behaviour (Hua *et al.*, 1998; Radhakrishnan *et al.*, 1998).

Of the four stathmin/OP18 phosphorylation sites, Ser63 is in the middle of H 1 of stathmin/OP18. This region has a strong tendency to form an α-helix in isolation and it is very likely that it will form an α-helix in the complex with tubulin. The fact that stathmin/OP18 does not possess a well-defined structure in isolation can explain how this residue is phosphorylated, since usually residues localized in secondary structure elements are not substrates of kinases.

We have identified a possible PPII helix with the motif PXXPXXPP between the N-terminus and the first helix. A PPII helix consists of a repeat of the motif $(PXX)_n$ and has been shown to mediate protein–protein interactions, such as in SH3 domains (for a review, see Williamson, 1994) or WW domains. The PPII helix postulated in stathmin/OP18 could be involved in binding to α-tubulin, although we have no evidence for that; it could be part of the signalling cascade that regulates stathmin/OP18 activity or, alternatively, be a binding site for a downstream effector of stathmin/OP18.

Stathmin/Op18 binds to tubulin through multiple binding sites

Our results show that the isolated helices H 1 and H 2 by themselves have no effect on tubulin polymerization at the concentrations tested, although they do bind to α-tubulin as demonstrated by chemical cross-linking. In combination, the effect on tubulin polymerization is indistinguishable from that of the holo-stathmin/OP18. It looks as if the binding of a single helix is not sufficient to interrupt polymerization. This could be due to a low binding affinity or because the interaction surface area covered on α-tubulin by only one helix is too small. The truncation (N+H 1) has some inhibitory activity on tubulin polymerization, albeit at a higher concentration than truncation (H 1+H 2) or holo-stathmin/OP18. This result is in agreement with the findings of Howell *et al.* (1999). These authors found that a truncated stathmin/OP18 without H 2 [their Δ100–147, similar to our (N+H 1)] binds tubulin poorly (0.5 mol of tubulin per mol of stathmin/OP18) and has low sequestering activity at pH 6.8, suggesting that tight binding is necessary for sequestration.

Altogether these results suggest that each stathmin/OP18 region binds to tubulin with weak affinity and it is the presence of two or more regions that results in a binding constant large enough to compete with tubulin polymerization effectively.

Model for the interaction between stathmin/OP18 and tubulin

For the interpretation of the cross-linking data we are only considering unique fragments, i.e. fragments derived from masses that unambiguously yield a single possible solution. The regions of stathmin/OP18 that are found to cross-link with α-tubulin are helix H 1 and helix H 2. No cross-links have been found with the N-terminus (residues 1–59) or the extreme C-terminus (residues 142–158, numbers include the nine residues added by the His tag). There are two regions of α-tubulin involved in the interaction with stathmin/OP18. The major region comprises the loops around α-helix 10 (Figure 7). Helix 10 of α-tubulin is located at the proposed minus end of the heterodimer (Mitchison, 1993; Fan *et al.*, 1996; Nogales *et al.*, 1998) interacting longitudinally with the β-tubulin of the following heterodimer. According to the high-resolution model of the MT by Nogales *et al.* (1999), a major zone of longitudinal interactions between the heterodimers encompasses residues 324–349 (helix 10) in α-tubulin. In fact, this is the ideal location to interrupt longitudinal heterodimer contact. The other region, identified unambiguously only with the truncation products (although it is found in one case as an ambiguous

assignment with the full-length stathmin/OP18), encompasses residues 155–162 [helix 4–strand 5 (H4–B5)] of α-tubulin. This loop is involved in lateral contacts (between two filaments) with helix 10 of the neighbouring α-tubulin molecule (Nogales *et al.*, 1999).

Our data suggest that there are different binding modes for the complex, depending on whether α-tubulin is bound to full-length stathmin/OP18 or its truncation products. As was pointed out before, higher order complexes (more than a 1:1 molar ratio) between stathmin/OP18 and α-tubulin are not formed with any of the truncation products of stathmin/OP18. In the full-length stathmin/OP18–α-tubulin complex our data place helices H 1 and H 2 at the minus end (i.e. around helix 10) of α-tubulin, presumably such that two heterodimers become linked (see Figure 8). The data from the truncated stathmin/OP18–α-tubulin complex place H 1 close to residues 155–163 (H4–B5) and presumably leave H 2 close to helix 10 as in the full-length complex. This indicates that H 1 has two possible binding sites on α-tubulin, one interrupting longitudinal contacts, the other lateral contacts.

We have not found any interactions with the N-terminus of stathmin/OP18. Since phosphorylation regulates stathmin/OP18 activity it must play a role in binding to tubulin. A possible explanation could be that the N-terminus binds to the highly modified C-terminal region of tubulin. Because of the complexity of the modifications of tubulin in MTs we would miss any C-terminal fragment that is modified by glycylation and/or glutamation, although we have taken into account possible detyrosination of the C-terminus. In fact, this might explain the masses that cannot be assigned to any cross-linked fragments.

Finally, we have not found any unique specific cross-linking with the β-tubulin subunit, as expected from the low percentage (<20%) of cross-linked product reported in the literature.

Higher order stathmin/OP18–tubulin complexes and the role of the N-terminus

Larsson *et al.* (1999) described the formation of higher order complexes of stathmin/OP18 with tubulin, which could be diluted out to a 1:2 molar ratio complex (the aforementioned T_2S complex). We find these higher order complexes in our cross-linking assays only with the full-length stathmin/OP18. Since the truncation (H 1+H 2) of stathmin/OP18 is fully active, indicating that the complex formed is stable but does not make higher order complexes, it can be assumed that the N-terminus [seemingly only in conjunction with the two helices, since the truncation (N+H 1) does not make higher order complexes either] is responsible for stable binding to the second molecule of tubulin. We propose that in the absence of the N-terminus, stathmin/OP18 binds to only one molecule of α-tubulin, at the top of the free tubulin heterodimer, thus preventing polymerization. In the presence of the N-terminus there could be a conformational rearrangement of stathmin/OP18 such that it is possible for H 1 to interact with a second molecule of α-tubulin (Figure 8). This is in agreement with the CD data showing a structural change in stathmin/OP18 when the N-terminal region and H 2 are present in the same molecule. Also, it agrees with the fact that we cannot find any cross-linking product involving

the N-terminus of stathmin/OP18. From our data the role of the T_2S complex *in vivo* is not clear: it could stabilize the tubulin–stathmin/OP18 complex, or simply improve the stoichiometry, i.e. make more efficient use of the amount of stathmin/OP18 in the cell for depleting the pool of tubulin available for polymerization and thus decreasing its concentration below the critical concentration for self-polymerization. The non-globular nature of stathmin/Op18 explains why it can interact with more than one tubulin molecule, as well as with structurally non-contiguous regions in α-tubulin.

Materials and methods

DNA constructs
DNA isolation and manipulations were performed using standard techniques. Stathmin/OP18 was derived from human cDNA (a gift from Søren S.L.Andersen). The full-length protein was expressed in *E.coli* BL21 with a His_6-tag derived from the vector pHat2 (Peranen *et al.*, 1996). The truncated proteins were constructed by using the polymerase chain reaction to amplify the DNA fragment of interest from the original full-length clone and cloning them into the *Nco*I–*Hin*dIII sites of the expression vector pHat2. The following protein fragments were amplified: for N+H 1: MASS...NNN; for H 1+H 2: KDLSL....ESKDPA; for H 1: KDLSL...NNN; for H 2: NNN...ESKDPA. All proteins (with the exception of the full-length protein and N+H 1) include the following 10 amino acids added by the His tag with the N-terminal methionine removed: SHHHHHHSMA. The full-length protein and the N+H 1 truncation are only elongated by the eight amino acids SHHHHHHS.

Protein purification
Wild-type and truncated stathmin/OP18 were expressed in *E.coli* BL21 and purified using either Ni–NTA resin (Qiagen, Germany) or Talon (Clontech, USA). For purification of the wild-type stathmin/OP18 the crude cell extract was heated to 90°C for 15 min prior to application to the affinity resin. The truncation products were not subjected to heat treatment. Non-specifically bound protein was removed by elution with 20 mM imidazole; the specifically bound protein was eluted with 250 mM imidazole, 300 mM NaCl in 50 mM PO_4 pH 7.0. The protein was then purified further over a S75 size-exclusion column (Pharmacia) in 150 mM NaCl, 50 mM PIPES pH 6.8. The identity of the purified protein was verified by mass spectrometry (MALDI-TOF). Protein concentration was determined by the Lowry method (Lowry *et al.*, 1951).

Mouse brain tubulin was prepared by two cycles of polymerization and depolymerization followed by chromatography on phosphocellulose (Mitchison and Kirschner, 1984). All procedures were scaled down appropriately. Seventeen mouse brains yielded ~4 mg of phosphocellulose pure tubulin. Bovine brain tubulin was isolated from calf brain in the manner described above and was a gift of the Karsenti and Hyman laboratories at the EMBL. The phosphocellulose pure fractions were subjected to an additional cycle of polymerization and depolymerization. Tubulin was stored at –80°C in BRB80 (20 mM K-PIPES pH 6.8, 0.25 mM EGTA, 0.25 mM $MgCl_2$) until use. Tubulin concentration was determined spectrophotometrically using an extinction coefficient of 1.2 mg^{-1} cm^2 at 278 nm (Detrich and Williams, 1978).

Cross-linking
For cross-linking studies 6.6 µM stathmin/OP18 and 11.62 µM mouse or bovine brain tubulin were incubated in 100 µl of BRB80 at 4°C for 1 h. Five microlitres of the zero-length cross-linker EDC (40 mM stock, 2 mM final; Pierce) were added and the sample was incubated at room temperature for 30 min. The reaction was quenched with 12 µl of hydroxylamine (100 mM stock, 10 mM final; Pierce). The samples were analysed by SDS–PAGE. The truncation products and the controls BSA and CheY were added at the same molar ratio.

Gel electrophoresis and Western blots
Gel electrophoresis was performed on 10 or 12% SDS–PAGE gels. Proteins were either stained with Coomassie Blue or immunoblotted. Proteins were transferred onto nitrocellulose filters in a semi-dry electroblotting apparatus (Trans-Blot semi-dry transfer cell; Bio-Rad). The blots were probed with a rabbit polyclonal stathmin/OP18 antibody directed against the peptide KKK...EERRK (a gift of Tony Ashford and

Tony Hyman) at 1:2000 dilution, a mouse monoclonal antibody against α-tubulin (N356; Amersham-Pharmacia Biotech) at a 1:1000 dilution and a mouse monoclonal antibody against β-tubulin (clone TUB 2.1; Sigma) at 1:2000 dilution. Bound antibodies were detected by chemiluminescence (ECL; Amersham International) with the appropriate secondary antibodies and exposure of the membranes to film (Kodak-XAR 5; Eastman Kodak Co.).

Microtubule assembly

Tubulin polymerization was monitored turbidimetrically at 350 nm in a SpectraMaxPlus UV spectrophotometer (Molecular Devices) thermostated at 37°C, using a 96 well microtitre plate and a 100 μl volume per well. For the data shown in Figure 5 each point is the average of two separate sets of experiments where each value was measured in duplicate. The reaction was carried out in BRB80 and 33% glycerol. Buffer and the appropriate amounts of stathmin/OP18 and its truncations were pre-heated to 37°C, then bovine tubulin was added at 5.8 mg/ml (58 μM) and the reaction was started by the addition of 1 μl of 100 mM GTP. The end point of polymerization was monitored and plotted against stathmin/OP18 concentration. Under these conditions polymerization took ~25 min.

CD measurements

The CD spectra were acquired in a JASCO-710 dichograph, using the continuous mode with 1 nm bandwidth, 1 s response and a scan speed of 50 nm/min. The samples were diluted appropriately and spectra recorded at 5°C. Each spectrum is the average of 10 scans. Helix content was estimated according to Chen *et al.* (1974):

$$\% \text{ helix} = \theta^{obs}_{222} \times 100/\theta^{hel}_{222} \times (1 - 2.57/l)$$

where θ^{obs}_{222} is the mean-residue ellipticity observed at 222 nm, θ^{hel}_{222} is the ellipticity of a peptide of infinite length with 100% helix population, taken as $-39\ 500\ \text{deg}^2\ \text{dmol}^{-1}$, and l is the number of peptide bonds.

A thermal denaturation spectrum was recorded for holo-stathmin/OP18, recording the ellipticity at 222 nm over a temperature range from 278 to 368K.

Peptides of the sequences YG**P**EF**P**LS**P**P and YG**P**EF**G**LS**P**P (control) were synthesized by Sigma-Genosys (Cambridge, UK). The molecular weight was confirmed by mass spectrometry and peptide purity was assessed by analytical HPLC. The tyrosine was added to the N-terminus to facilitate peptide concentration determination. An extinction coefficient ε of 1400 $M^{-1}cm^{-1}$ at 274 nm was used to calculate peptide concentration. The near-UV CD spectra were recorded in the range 190–250 nm in a 0.01 cm pathlength cuvette at 4°C with the above described settings. Peptide concentrations were 800 μM in 50 mM phosphate buffer at pH 6.8.

Purification of the α-tubulin–stathmin/OP18 complex and mass spectrometry

The stathmin/OP18–tubulin complexes from mouse brain tubulin were purified by SDS–PAGE. The bands corresponding to the α-tubulin–stathmin/OP18 complex were excised from the unstained gels and electroeluted (Centrilutor, Amicon) in 0.1% SDS, 50 mM borate pH 9.0, 10% methanol. The SDS was removed by precipitating the eluate in ice-cold ethanol overnight. The complex was dissolved in 50 mM Tris pH 8.0, 1 mM EDTA for digestion. A total of 18–37 pmol of sample were digested by either trypsin or Endo-LysC (sequencing grade; Boehringer Mannheim) at a ratio of 20:1 (w:w) overnight at 37°C. Samples were prepared and analysed as described in Jensen *et al.* (1996). The samples were analysed by MALDI-TOF MS on a Bruker RELEX mass spectrometer (Bruker Daltonics). Mass spectra were acquired as the sum of 100–250 ion signals. Monoisotopic masses were assigned using the software LaserOne (developed by the group of M.M. at the EMBL, Heidelberg, Germany). Self-cross-linked and uncross-linked mouse tubulin and stathmin/OP18 were analysed as controls.

Acknowledgements

References

Andersen,S.S. (1999) Balanced regulation of microtubule dynamics during the cell cycle: a contemporary view. *BioEssays*, **21**, 53–60.

Belmont,L.D. and Mitchison,T.J. (1996) Indentification of a protein that interacts with tubulin dimers and increases the catastrophe rate of microtubules. *Cell*, **84**, 623–631.

Chen,Y.-H., Yang,J.T. and Chau,K.H. (1974) Determination of the helix and β form of proteins in aqueous solution by circular dichroism. *Biochemistry*, **13**, 3350–3359.

Cohen,S.L. and Chait,B.T. (1996) Influence of matrix solution conditions on the MALDI-MS analysis of peptides and proteins. *Anal. Chem.*, **68**, 31–37.

Cole,N.B. and Lippincott-Schwartz,J. (1995) Organization of organelles and membrane traffic by microtubules. *Curr. Opin. Cell Biol.*, **7**, 55–64.

Curmi,P.A., Maucuer,A., Asselin,S., Lecourtois,M., Chaffotte,A., Schmitter,J.-M. and Sobel,A. (1994) Molecular characterization of human stathmin expressen in *Escherichia coli*: site-directed mutagenesis of two phosphorylatable serines (Ser-25 and Ser-63). *Biochem. J.*, **300**, 331–338.

Curmi,P.A., Andersen,S.S.L., Lachkart,S., Gavet,O., Karsenti,E., Knossow,M.A. and Sobel,A. (1997) The stathmin/tubulin interaction *in vitro*. *J. Biol. Chem.*, **272**, 25029–25036.

Detrich,H.W.,III and Williams,R.C. (1978) Reversible dissociation of the αβ dimer of tubulin from bovine brain. *Biochemistry*, **17**, 3900–3907.

Drechsel,D.N., Hyman,A.A., Cobb,M.H. and Kirschner,M.W. (1992) Modulation of the dynamic instability of tubulin assembly by the microtubule-associated protein τ. *Mol. Biol. Cell*, **3**, 1141–1154.

Fan,J., Griffiths,A.D., Lockhart,A., Cross,R.A. and Amos,L.A. (1996) Microtubule minus ends can be labelled with a phage display antibody specific to α-tubulin. *J. Mol. Biol.*, **259**, 325–330.

Hirokawa,N. (1994) Microtubule organization and dynamics dependent on microtubule-associated proteins. *Curr. Opin. Cell Biol.*, **6**, 74–81.

Horwitz,S.B., Shen,H.-J., He,L., Dittmar,P., Neef,R., Chen,J. and Schubart,U.K. (1997) The microtubule-destabilizing activity of metablastin (p19) is controlled by phosphorylation. *J. Biol. Chem.*, **272**, 8129–8132.

Howell,B., Larsson,N., Gullberg,M. and Cassimeris,L. (1999) Dissociation of the tubulin-sequestering and microtubule catastrophe-promoting activities of oncoprotein 18/stathmin. *Mol. Biol. Cell*, **10**, 105–118.

Hua,Q.X., Jia,W.H., Bullock,B.P., Habener,J.F. and Weiss,M.A. (1998) Transcriptional activator–coactivator recognition: nascent folding of a kinase-inducible transactivation domain predicts its structure on coactivator binding. *Biochemistry*, **37**, 5858–5866.

Jensen,O.N., Podtelejnikov,A. and Mann,M. (1996) Delayed extraction improves specificity in database searches by matrix-assisted laser desorption/ionization peptide maps. *Rapid Commun. Mass Spectrom.*, **10**, 1371–1378.

Jourdain,L., Curmi,P.A., Sobel,A., Pantaloni,D. and Carlier,M.-F. (1997) Stathmin: a tubulin-sequestering protein which forms a ternary T_2S complex with two tubulin molecules. *Biochemistry*, **36**, 10817–10821.

Kraulis,P.J. (1991) MOLSCRIPT: a program to produce both detailed and schematic plots of proteins. *J. Appl. Crystallogr.*, **24**, 946–950.

Lacroix,E., Viguera,A.R. and Serrano,L. (1998) Elucidating the folding problem of α-helices: local motifs, long-range electrostatics, ionic-strength dependence and prediction of NMR parameters. *J. Mol. Biol.*, **284**, 173–191.

Larsson,N., Marklund,U., Gradin,H.M., Brattsand,G. and Gullberg,M. (1997) Control of microtubule dynamics by oncoprotein 18: dissection of the regulatory role of multisite phosphorylation during mitosis. *Mol. Cell. Biol.*, **17**, 5530–5539.

Larsson,N., Segerman,B., Gradin,H.M., Wandzioch,E., Cassimeris,L. and Gullberg,M. (1999) Mutations of oncoprotein 18/stathmin identify tubulin-directed regulatory activities distinct from tubulin association. *Mol. Cell. Biol.*, **19**, 2242–2250.

Lowry,O.H., Rosebrough,N.J., Farr,A.L. and Randall,R.J. (1951) Protein measurement with the folin phenol reagent. *J. Biol. Chem.*, **193**, 265–275.

Lupas,A., Van Dyke,M. and Stock,J. (1991) Predicting coiled coils from protein sequences. *Science*, **252**, 1162–1164.

Marklund,U., Brattsand,G., Ostermann,O., Ohlsson,P.I. and Gullberg,M. (1993) Multiple signal transduction pathways induce phosphorylation of serines 16, 25 and 38 of oncoprotein 18 in T lymphocytes. *J. Biol. Chem.*, **268**, 25671–25680.

Maucuer,A., Moreau,J., Mechali,M. and Sobel,A. (1993) Stathmin gene

family: phylogenetic conservation and developmental regulation in *Xenopus*. *J. Biol. Chem.*, **1993**, 16420–16429.

Maucuer,A., Camonis,J.H. and Sobel,A. (1995) Stathmin interaction with a putative kinase and coiled-coil forming protein domains. *Proc. Natl Acad. Sci. USA*, **92**, 3100–3104.

Mitchison,T.J. (1993) Localization of an exchangeable GTP binding site at the plus end of microtubules. *Science*, **261**, 1044–1047.

Mitchison,T. and Kirschner,M. (1984) Dynamic instability of microtubule growth. *Nature*, **312**, 237–242.

Moreno,F.J., Bagnat,M., Lim,F. and Avila,J. (1999) OP18/stathmin binds near the C-terminus of tubulin and facilitates GTP binding. *Eur. J. Biochem.*, **262**, 557–562.

Munoz,V. and Serrano,L. (1994) Elucidating the folding problem of helical peptides using empirical parameters. *Nature Struct. Biol.*, **1**, 399–409.

Nogales,E., Wolf,S.G. and Downing,K.H. (1998) Structure of the αβ tubulin dimer by electron crystallography. *Nature*, **391**, 199–203.

Nogales,E., Whittaker,M., Milligan,R.A. and Downing,K.H. (1999) High-resolution model of the microtubule. *Cell*, **96**, 79–88.

Peranen,J., Rikkonen,M., Hyvonen,M. and Kaariainen,L. (1996) T7 vectors with modified T7lac promoter for expression of proteins in *Escherichia coli. Anal. Biochem.*, **236**, 371–373.

Pisabarro,M.T. and Serrano,L. (1996) Rational design of specific high-affinity peptide ligands for the Abl-Sh3 domain. *Biochemistry*, **35**, 10634–10640.

Radhakrishnan,I., Perez-Alvarado,G.C., Dyson,H.J. and Wright,P.E. (1998) Conformational preferences in the Ser133-phosphorylated and non-phosphorylated forms of the kinase inducible transactivation domain of CREB. *FEBS Lett.*, **430**, 317–322.

Redeker,V., Levilliers,N., Schmitter,J.M., Le Caer,J.P., Rossier,J., Adoutte,A. and Bre,M.H. (1994) Polyglycylation of tubulin: a posttranslational modification in axonemal microtubules. *Science*, **266**, 1688–1691.

Redeker,V., Rossier,J. and Frankfurter,A. (1998) Posttranslational modifications of the C-terminus of α-tubulin in adult rat brain: α4 is glutamylated at two residues. *Biochemistry*, **37**, 14838–14844.

Rost,B., Sander,C. and Schneider,R. (1994) PHD–an automatic mail server for protein secondary structure prediction. *Comput. Appl. Biosci.*, **10**, 53–60.

Viguera,A.R., Arrondo,J.L.R., Musaccio,A., Saraste,M. and Serrano,L. (1994) Characterization of the interaction of natural proline-rich peptides with five different SH3 domains. *Biochemistry*, **33**, 10925–10933.

Villasante,A., Wang,D., Dobner,P., Dolph,P., Lewis,S.A. and Cowan,N.J. (1986) Six mouse α-tubulin mRNAs encode five distinct isotypes: testis-specific expression of two sister genes. *Mol. Cell. Biol.*, **6**, 2409–2419.

Vinh,J., Langridge,J.I., Bre,M.H., Levilliers,N., Redeker,V., Loyaux,D. and Rossier,J. (1999) Structural characterization by tandem mass spectrometry of the posttranslational polyglycylation of tubulin. *Biochemistry*, **38**, 3133–3139.

Williamson,M.P. (1994) The structure and function of proline-rich regions in proteins. *Biochem. J.*, **297**, 249–260.